MODELING OF NOM-FACILITATED PAH TRANSPORT THROUGH LOW-f_{oc} SEDIMENT

By William P. Johnson,[1] Gary L. Amy,[2] and Steven C. Chapra[3]

ABSTRACT: A finite-difference model was developed to more closely examine the observation that polycyclic aromatic hydrocarbon (PAH) transfer to and from low-organic-carbon aquifer sediment and aqueous natural organic matter (NOM) apparently occurred uninhibited by kinetic limitations during facilitated-transport and enhanced-desorption experiments performed in laboratory columns. The model accounted for advection, dispersion, and mass transfer between the various phases comprising the system; i.e., distribution of PAH between water and sediment and water and NOM, and distribution of NOM between water and sediment. The model was run using mass-transfer coefficients based on the equilibrium constants derived from experimental data and compared against the literature. Successful reproduction of the experimentally observed facilitated-transport and enhanced-desorption curves indicated that our physical system was free of kinetic limitations and was describable by the equilibrium constants comprising the system.

INTRODUCTION

Polycyclic aromatic hydrocarbons (PAH) are ubiquitous by-products of the incomplete combustion of carbon-based substances. Many PAH are known carcinogens. PAH are widely distributed in soil and marine sediments, and PAH contamination near major urban and industrial sources is evident (Baum 1978). PAH are relatively insoluble in water and tend to attenuate in soils and sediments. Recently, the ability of mobile colloids such as natural organic matter (NOM) to bind and transport PAH has been examined (Liu and Amy 1993; Schlautman and Morgan 1993; Backhus and Gschwend 1990). In Johnson and Amy (1995), it was shown that PAH interactions with NOM and sediment may occur quickly, so that PAH moves freely from NOM to sediment and from sediment to NOM, as conditions change within a system of PAH, NOM, and sediment. For instance, it was observed that complete NOM breakthrough can precede the initiation of PAH breakthrough even when NOM and PAH are preequilibrated, suggesting that PAH freely leaves its bound position with NOM to move to PAH-free sediment in the initial stage of a facilitation experiment. This free movement of PAH from NOM to sediment is counterintuitive given the high affinity between PAH and NOM relative to that between PAH and low organic carbon (f_{oc}) sediment. As well, PAH is observed to readily leave its position on PAH-loaded sediment to move to PAH-free NOM during enhanced-desorption experiments, as evidenced by solubility enhancement of PAH to many times its normal water solubility upon introduction of NOM into the sediment column. These phenomena are presumably driven by interaction of the binary equilibrium constants quantifying the affinities between the various phases in the system. Comparison of our experimentally derived association constants for PAH with NOM to the existing literature indicated that our system was at equilibrium. However, given the large quantity of literature that describes nonequilibrium sorption and desorption of hydrophobic compounds to soil (Brusseau and Reid 1991; Brusseau et al. 1991), equilibrium mass transfer in our system was suspect. A model was developed, therefore, to investigate whether our experimental observations could be reproduced by a model accounting for advection, dispersion, and mass transfer between phases based on the equilibrium constants comprising the system.

Models that examine one-dimensional transport of a solute in ground water are numerous. Variations among them include the ability to account for nonlinear sorption (Grove and Stollenwerk 1984), rate-limited sorption (Brusseau et al. 1991), and general physical or chemical nonequilibrium (Parker and van Genuchten 1984), in addition to the effects of advection and dispersion. Models developed to simulate the transport of a solute in the presence of a potential facilitating agent are few in number. Mills et al. (1991) introduced a conceptual colloids-metal transport model to simulate the facilitation of metal transport in the presence of colloids. Magee et al. (1991) presented a modification of the conventional formulation of the retardation factor that accounts for the effect of a mobile carrier on the retardation of a contaminant. Corapcioglu and Jiang (1992), developed a one-dimensional model based on equilibration of the binary interactions that comprise a solute-colloid-sediment system, a model that is conceptually similar to ours but was applied only to a facilitated-transport scenario (as opposed to enhanced desorption) and to only one set of experimental data. Our model, based on the theoretical development presented in Enfield et al. (1989), was developed to elucidate the mechanisms governing our experimental observations, which included enhanced desorption as well as facilitated transport, and spanned a variety of PAH-NOM and PAH-sediment affinities.

Fig. 1 is a schematic diagram of our model, which is governed by the following five differential equations derived by mass balance:

$$\frac{\partial c_a}{\partial t} = D_a \cdot \frac{\partial^2 c_a}{\partial x^2} - v_a \cdot \frac{\partial c_a}{\partial x} - KPAH_{a-o} \cdot c_a - KPAH_{a-s} \cdot c_a + KPAH_{o-a} \cdot c_o \cdot cnom_a + KPAH_{s-a} \cdot \frac{(1-n) \cdot \rho_s \cdot c_s}{(\theta \cdot \rho_a)} \quad (1)$$

$$\frac{\partial cnom_a}{\partial t} = D_o \cdot \frac{\partial^2 cnom_a}{\partial x^2} - v_o \cdot \frac{\partial cnom_a}{\partial x} - KNOM_{o-s} \cdot cnom_a + KNOM_{s-o} \cdot \frac{(1-n) \cdot \rho_s \cdot cnom_s}{\theta \cdot \rho_a} \quad (2)$$

$$\frac{\partial (c_o \cdot cnom_a)}{\partial t} = D_o \cdot \frac{\partial^2 (c_o \cdot cnom_a)}{\partial x^2} - v_o \cdot \frac{\partial (c_o \cdot cnom_a)}{\partial x} - KPAH_{o-a} \cdot c_o \cdot cnom_a + KPAH_{a-o} \cdot c_a \quad (3)$$

[1]Res. Sci., Dept. of Chem. and Envir. Engrg./Dept. of Hydro. and Water Resour., Univ. of Arizona, Tuscon, AZ 85721.

[2]Prof., Dept. of Civ. and Envir. Engrg., Univ. of Colorado at Boulder, Boulder, CO 80309.

[3]Prof., Dept. of Civ. and Envir. Engrg., Univ. of Colorado at Boulder, Boulder, CO.

Note. Discussion open until November 1, 1995. To extend the closing date one month, a written request must be filed with the ASCE Manager of Journals. The manuscript for this paper was submitted for review and possible publication on October 11, 1993. This paper is part of the ***Journal of Environmental Engineering***, Vol. 121, No. 6, June, 1995. ©ASCE, ISSN 0733-9372/95/0006-0438–0446/$2.00 + $.25 per page. Paper No. 7129.

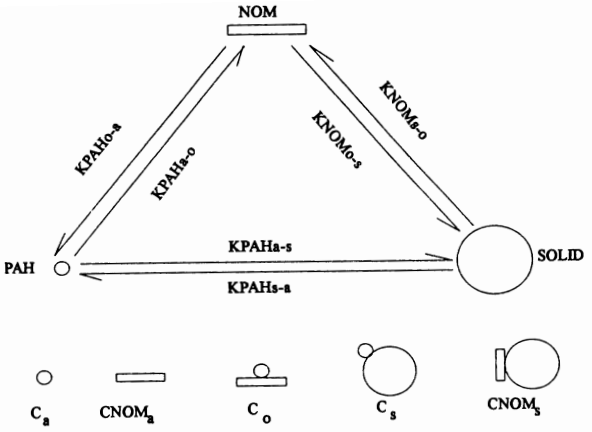

FIG. 1. Schematic Diagram of Components of System

$$\frac{\partial cnom_s}{\partial t} = -KNOM_{s-o} \cdot cnom_s + KNOM_{o-s} \cdot \frac{\theta \cdot \rho_a \cdot cnom_a}{(1 - n) \cdot \rho_s} \tag{4}$$

$$\frac{\partial c_s}{\partial t} = -KPAH_{s-a} \cdot c_s + KPAH_{a-s} \cdot \frac{\theta \cdot \rho_a \cdot c_a}{(1 - n) \cdot \rho_s} \tag{5}$$

where REV = representative elemental volume; θ = volumetric water content of REV (L^3water/L^3REV); ρ_a = density of water (Mwater/L^3water); ρ_s = density of sediment (Msediment/L^3sediment); n = porosity of sediment (L^3voids/L^3REV); v_a = pore velocity of water ($LREV/T$); D_a = dispersion coefficient of free PAH in aqueous phase (L^2REV/T); v_o = velocity of mobile organic phase ($LREV/T$); D_o = dispersion coefficient of mobile organic phase (L^2REV/T); c_a = concentration of PAH in water (mass PAH/mass water); $cnom_a$ = concentration of NOM in water (mass NOM/mass water); c_o = concentration of PAH in mobile organic matter (mass PAH/mass NOM); c_s = concentration of PAH on sediment (mass PAH/mass sediment); and $cnom_s$ = concentration of NOM on sediment (mass NOM/mass sediment).

Notice that these concentrations are on a mass-per-mass basis. To convert to mass per volume, multiply by mass per volume for water, which for mg/mL is unity in our system. The mass-transfer coefficients (MTC), with units of inverse time ($1/T$), are given as follows: $KPAH_{a-o}$ = MTC of PAH from the free aqueous phase to the mobile organic phase; $KPAH_{o-a}$ = MTC of PAH from the mobile organic phase to the free aqueous phase; $KPAH_{a-s}$ = MTC of PAH from the free aqueous phase to the sediment phase; $KPAH_{s-a}$ = MTC of PAH from the sediment phase to the free aqueous phase; $KNOM_{o-s}$ = MTC of NOM from the mobile organic phase to the stationary sediment phase; and $KNOM_{s-o}$ = MTC of NOM from the stationary sediment phase to the mobile organic phase.

Results from two types of experiments were reproduced by our model: facilitation and enhanced-desorption experiments. In the facilitation experiments, comparison was made between the breakthrough curve (BTC) for transport of PAH alone through a particular sediment, and the BTC for the same PAH preequilibrated with an NOM through the same sediment. The difference between these BTCs indicated the ability of the NOM to facilitate the transport of the PAH. In enhanced-desorption experiments, comparison was made between the eluent curve for desorption of a PAH from a PAH-contaminated sediment by NOM-free water, and the eluent curve for desorption by an NOM solution. The difference between these curves indicated the ability of the NOM to enhance the desorption of the PAH from the sediment.

MATERIALS AND METHODS

Experimental

The PAH modeled in this study is benz(a)anthracene, B(a)A, which has a solubility of 7.1 μg/L (May, 1980), and a log K_{ow} of 5.6 (Callahan et al. 1979). Suwannee River Humic Acid (SRHA) and Soil Humic Acid (SHA) were obtained from the International Humic Substances Society and were used to facilitate the transport and enhance the desorption of B(a)A through (and from) a variety of aquifer sediments as described in Johnson and Amy (1995). B(a)A transport was observed to be more strongly affected by the presence of aqueous SHA relative to aqueous SRHA, as is predictable from the fact that soil-derived humic materials generally display higher molecular weights relative to aquatic humic substances. The two sediments modeled in this study are referred to as quartz sediment [% organic carbon (OC) = 0.0004; porosity = 0.49; and specific surface area = 0.085 m^2/g], which was obtained commercially, and nonmagnetic sediment (%OC = 0.0003; porosity = 0.43; specific surface area = 0.40 m^2/g), which is derived from natural aquifer sediment as described in Johnson and Amy (1995). The surface areas were measured by multiple-point BET (Brunauer et al. 1938) nitrogen gas adsorption (by Dave Rutherford, U.S. Geological Survey). The organic carbon contents were measured by Huffman Laboratories, Golden, Colorado.

Model

The mass-transfer coefficients for PAH transfer from the aqueous phase to the mobile organic phase and back are normalized by the concentration of mobile NOM, in order to relate the mass transfer of PAH to the amount of NOM present. This approach assumes that NOM affinity for PAH is independent of NOM concentration, and that the ability of the NOM to bind PAH is unaltered by dilution or concentration. We continue to use this assumption in our model because we consider these dilution or concentration effects on NOM-PAH affinity to be secondary to their overall effects on mass transfer.

The model computes and records mass adsorbed during simulation of adsorption of PAH alone and during simulation of facilitation of PAH by NOM. Mass adsorbed is determined by integration of the area above the BTC from background concentration to equilibrium concentration over time. An independent measure of mass adsorbed is also obtained by adding the concentration of PAH on sediment across all segments for the last time step (after equilibrium is reached). Comparison of these two estimates of adsorbed mass is made to check the mass balance of the model in terms of sediment sorption of PAH. Mass not adsorbed (mass passed through the column) is calculated by integration below the BTC, and this mass plus the mass adsorbed must equal total mass flux through the system in order to ensure mass balance. The governing equations were solved numerically by a Crank-Nicholson scheme. Initial and boundary conditions used are given in Table 1.

PARAMETERS

Physical Parameters

Pore-water velocity, v_a, values were determined by dividing the volumetric flux, $Q(L^3/T)$, by the cross-sectional area of the column interior, $A(L^2)$, and the sediment volumetric water content, $\theta(L^3/L^3)$, as follows:

$$v_a = \frac{Q}{A \cdot \theta} = \frac{L^3\text{water}}{T} \cdot \frac{1}{L^2REV} \cdot \frac{L^3REV}{L^3\text{water}} = \frac{LREV}{T} \tag{6}$$

TABLE 1. Initial and Boundary Conditions

Condition (1)	Location (2)	PAH adsorption (3)	PAH desorption (4)	Facilitated transport (5)	Enhanced desorption (6)
$c_a(x, t)$	$x = 0$	7.1E − 08	0.0	$\frac{1}{1 + K_p \cdot cnom_a} \cdot 7.1E - 08$	0.0
$\frac{\partial c_a(x, t)}{\partial x}$	$x = L$	0.0	0.0	0.0	0.0
$cnom_a(x, t)$	$x = 0$	0.0	0.0	2.0×10^{-5}	2.0E − 05
$\frac{\partial cnom_a(x, t)}{\partial x}$	$x = L$	0.0	0.0	0.0	0.0
$c_o(x, t)$	$x = 0$	0.0	0.0	$\frac{K_p \cdot cnom_a}{1 + K_p \cdot cnom_a} \cdot 7.1E - 08$	0.0
$\frac{\partial c_o(x)}{\partial x}$	$x = L$	0.0	0.0	0.0	0.0
$c_a(x, t)$	$t = 0$	0.0	7.1E − 08	0.0	7.1E − 08
$cnom_a(x, t)$	$t = 0$	0.0	0.0	0.0	0.0
$c_o(x, t)$	$t = 0$	0.0	0.0	0.0	0.0
$c_s(x, t)$	$t = 0$	0.0	c_s equilibrium	0.0	c_s equilibrium
$cnom_s(x, t)$	$t = 0$	0.0	0.0	0.0	0.0

where REV = representative elementary volume.

Numerical dispersion (E_{num}) is an undesirable added dispersion that occurs due to the use of a backward difference for the first derivative that quantifies solute advection (Thomann and Mueller 1987).

$$E_{num} = v_a \cdot \Delta x \cdot \left[\frac{1}{2} - \frac{v \cdot \Delta t}{2 \cdot \Delta x}\right] \tag{7}$$

E_{num} should be minimized in order to avoid adverse effects of the numerical approximation on model results. For a backward difference, $E_{num} = 0$ when $\Delta t = \Delta x / v_a$, where v_a = water velocity (cm/min); Δt = time step (min); and Δx = segment length (cm). The value for Δt that results in $E_{num} = 0$ is determined from the chosen Δx and the other parameters in the previous equation, and is given in Table 2.

Bulk density, ρ_b, values were obtained from an average of five measurements, performed by measuring the mass of a known volume of sediment (M/L^3)(sed/REV). Sediment porosity was determined by the following formulation:

$$n = \left(1 - \frac{\rho_b}{\rho_s}\right) = 1 - \frac{\frac{M\text{sed}}{L^3 REV}}{\frac{M\text{sed}}{L^3\text{sed}}} = 1 - \frac{L^3\text{sed}}{L^3 REV} = \frac{L^3\text{voids}}{L^3 REV} \tag{8}$$

where ρ_s = sediment density (2.65 gm/cm^3). The volumetric water content was set equal to porosity in our simulations.

Solute dispersion was determined by entering data from conservative tracer experiments into CXTFIT, a nonlinear least-squares curve-fitting model by Parker and van Genuchten (1984), which can be used to determine the optimal characterization of experimental data by an advection-dispersion equation that includes equilibrium or nonequilibrium sorption. CXTFIT was used to determine the dispersion coefficient of the tracer. In multiple runs, it was observed that our model was relatively insensitive to changes in D_a or D_o, even by a factor of 10. This observation, combined with the fact that our system is highly advective, indicates that setting D_a and D_o equal to the dispersion coefficient of the tracer exerted negligible effect on the overall results.

Chemical Parameters

The ratios of the mass-transfer coefficients, under equilibrium conditions, can be determined from the equilibrium-distribution and partition constants, developed as follows. At equilibrium, mass transfer in both directions is equal, i.e.

$$c_s \cdot KPAH_{s-a} \cdot (1 - n) \cdot \rho_s = c_a \cdot KPAH_{a-s} \cdot \theta \cdot \rho_a \tag{9}$$

Rearranging gives the ratio of PAH on sediment to PAH in free aqueous phase, which is the equilibrium-distribution coefficient for PAH between water and sediment, as follows:

$$\frac{c_s}{c_a} = \frac{KPAH_{a-s} \cdot \theta \cdot \rho_a}{KPAH_{s-a} \cdot (1 - n) \cdot \rho_s} = K_d \tag{10}$$

Likewise, for the other interactions

$$\frac{c_o \cdot cnom_a}{c_a} = \frac{KPAH_{a-o}}{KPAH_{o-a}} = K_p \cdot cnom_a \tag{11}$$

$$\frac{cnom_s}{cnom_a} = \frac{KNOM_{o-s} \cdot \theta \cdot \rho_a}{KNOM_{s-o} \cdot (1 - n) \cdot \rho_s} = K_n \tag{12}$$

where K_d = equilibrium-distribution coefficient for PAH between water and sediment; K_p = equilibrium-partition coefficient for PAH between water and NOM; and K_n = equilibrium-distribution coefficient for NOM between water and sediment. Rearranging, we obtain the following:

TABLE 2. Physical Parameters of Sediments for Numerical Approximation

Sediment (1)	Q cm^3REV/min (2)	A cm^2REV (3)	v_a cmREV/min (4)	Δx (cm) (5)	Δt (min) (6)	ρ_b gmsed/cm^3REV (7)	ρ_s gmsed/cm^{3}sed (8)	n cm^{3}voids/cm^3REV (9)	D_a cm^2REV/min (10)
Quartz	1.0	$\pi \cdot (0.95)^2$	0.73	0.15	0.21	1.36	2.65	0.49	0.03
Nonmagnetic	1.0	$\pi \cdot (0.95)^2$	0.82	0.15	0.18	1.51	2.65	0.43	0.04

$$\frac{KPAH_{a-s}}{KPAH_{s-a}} = K_d \cdot \frac{(1 - n) \cdot \rho_s}{\theta \cdot \rho_a} \quad (13)$$

$$\frac{KPAH_{a-o}}{KPAH_{o-a}} = K_p \cdot cnom_a \quad (14)$$

$$\frac{KNOM_{o-s}}{KNOM_{s-o}} = K_n \cdot \frac{(1 - n) \cdot \rho_s}{\theta \cdot \rho_a} \quad (15)$$

Thus the ratios of the mass-transfer coefficients are obtained from equilibrium constants K_p, K_d, and K_n. These constants were estimated from the experimental data as described in Johnson and Amy (1995), and are included in Table 3.

Influent values of c_a and c_o were determined from the following relation:

$$\frac{\text{mass}c_a}{\text{mass}c_{\text{total}}} = \frac{1}{1 + K_p \cdot cnom_a} \quad (16)$$

which describes the fraction of PAH in the free aqueous phase (c_a) relative to total PAH in the aqueous phase ($c_{\text{total}} = c_a + K_p \cdot cnom_a \cdot c_o$), where c_{total} is comprised of both free and NOM-bound PAH in the aqueous phase.

CHARACTERIZATION AS LINEAR ISOTHERMS

Mass transfer between two phases is governed by the ratio of the mass-transfer coefficients that quantify mass transfer in each direction. Because these mass-transfer coefficients are constant, the assumption is therefore made that the net–mass-transfer process is quantifiable by a single coefficient. A mass-transfer process that is quantified by a single constant can also be said to yield a linear isotherm. Three types of interactions, PAH-NOM, PAH-sediment, and NOM-sediment interactions, comprise our system. The appropriateness of characterizing these interactions with linear isotherms will now be briefly discussed.

PAH-NOM interactions are hydrophobic in nature and are describable by a linear isotherm (Schlautman and Morgan 1993; Backhus 1990; Gauthier et al. 1986; Chiou et al. 1986). PAH-sediment interactions are hydrophobically driven, and are also describable by a linear isotherm (Backhus and Gschwend 1990; Chiou et al. 1985; Karickhoff et al. 1979). NOM-sediment interactions are less easily characterized than the other two interactions because they are comprised of multiple mechanisms, including hydrophobic bonding and ligand exchange. NOM-sediment interactions yield either linear or nonlinear isotherms depending upon the dominance of a particular mechanism. The dominance of one binding mechanism over the other is dependent upon solution conditions such as pH and ionic strength (Schlautman 1992). NOM-sediment interactions were modeled by Jardine et al. (1992) to simulate laboratory column experiments performed by Dunnivant et al. (1992). Jardine et al. (1992) found that for high-influent dissolved organic carbon (DOC) concentrations (i.e., DOC > 10 mg/L, BTCs were adequately modeled as two-site nonlinear-adsorption processes, and DOC interactions with both sites were time-dependent. However, for influent DOC concentrations with DOC < 10 mg/L, BTCs were successfully modeled as a one-site, linear time-dependent adsorption process. In our experiments, sorption of NOM to sediment was low to nil. We chose to approximate NOM-sediment interaction in our system by a linear isotherm. Given that our influent NOM concentrations of 20 mg/L correspond to a DOC of about 10 mg/L on a carbon basis, the results of Jardine et al. (1992) suggest the appropriateness of this approximation.

MODEL RESULTS

The ratios and magnitudes of the mass-transfer coefficients that were input into the model are shown in Table 4. The corresponding model BTCs for sorption of B(a)A alone and facilitation of B(a)A by SRHA and SHA for both quartz and nonmagnetic sediment are shown in Figs. 2–5 along with experimental BTCs for comparison. The figures show c/c_0, which is the effluent concentration divided by the influent concentration on the vertical axis. Time, measured in pore volumes, which is the average residence time of a tracer in the column, is shown on the horizontal axis. Facilitation is recognized in the speeding of breakthrough, and is observed to be more effective for SHA than for SRHA. Dashed lines in Figs. 2 and 4 show curves obtained from mass-transfer coefficients that were determined from K_p values estimated from experiments performed on quartz and nonmagnetic sediments. The solid curves representing mass-transfer coefficients that were determined from the average of the two selected values. Figs. 3 and 5 show the sensitivity of the BTCs to increase and decrease of the mass-transfer coefficients by one order of magnitude. In Figs. 3 and 5, N = magnitude of PAH-NOM mass-transfer coefficients the same as those in Figs. 2 and 4, respectively; H = magnitude 10 times greater than N; and L = magnitude one-tenth of N. Curves achieving relatively quick breakthrough depict B(a)A-SHA interaction. Curves showing relatively slower breakthrough correspond to B(a)A-SRHA interaction. Both figures show the relative insensitivity of the model to mass-transfer–coefficient magnitude beyond that necessary to attain equilibrium.

Model simulations were also performed for desorption of B(a)A alone, and enhanced desorption of B(a)A by SRHA and SHA, from both quartz and nonmagnetic sediment. These results (Figs. 6–9), which are in the same format as the previously discussed Figs. 2–5, compare favorably with experimental results. Enhanced desorption is recognized in rise of the eluent curve above $c/c_0 = 1$, due to enhancement of PAH solubility above that in water alone. SHA is observed to enhance B(a)A solubility more effectively than SRHA.

TABLE 3. Mass-Transfer–Coefficient Ratios from Equilibrium Coefficients

Sediment (1)	Solute (2)	K_d (3)	$\frac{KPAH_{a-s}}{KPAH_{s-a}}$ (4)	K_n (5)	$\frac{KNOM_{o-s}}{KNOM_{s-a}}$ (6)	K_p (7)	$\frac{KPAH_{a-o}}{KPAH_{o-a}}$ (8)
Quartz	B(a)A	15.20	42.55	—	—	—	—
	SHA	—	—	0.00	0.00	—	—
	SRHA	—	—	0.00	0.00	—	—
	B(a)A + SHA	—	—	—	—	1.84E + 05	3.68
	B(a)A + SRHA	—	—	—	—	3.07E + 04	0.61
Nonmagnetic	B(a)A	6.01	21.11	—	—	—	—
	SHA	—	—	0.44	1.56	—	—
	SRHA	—	—	0.00	0.00	—	—
	B(a)A + SHA	—	—	—	—	3.42E + 05	6.84
	B(a)A + SRHA	—	—	—	—	1.35E + 04	0.27

TABLE 4. Mass-Transfer Ratios and Magnitudes for Model Simulations

Sediment (1)	Solute (2)	$\frac{KPAH_{a-s}}{KPAH_{s-a}}$ (3)	Magnetic (4)	$\frac{KNOM_{o-s}}{KNOM_{s-a}}$ (5)	Magnetic (6)	$\frac{KPAH_{a-o}}{KPAH_{o-a}}$ (7)	Magnetic (8)
Quartz	B(a)A	42.55/1.0	(4.0E − 03)/(4.0E − 03)	—	—	—	—
	SHA	—	—	0.0	—	—	—
	SRHA	—	—	0.0	—	—	—
	B(a)A + SHA	—	—	—	—	3.68/1.0	(E − 01)/(E − 01)
	B(a)A + SRHA	—	—	—	0.614/1.0	(E − 00)/(E − 00)	
Nonmagnetic	B(a)A	21.11/1.0	(7.5E − 03)/(6.0E − 03)	—	—	—	—
	SHA	—	—	1.56/1.0	(1.7E − 02)/(1.6E − 02)	—	—
	SRHA	—	—	0.0	—	—	—
	B(a)A + SHA	—	—	—	—	6.84/1.0	(E − 01)/(E − 01)
	B(a)A + SRHA	—	—	—	—	0.27/1.0	(E − 00)/(E − 00)

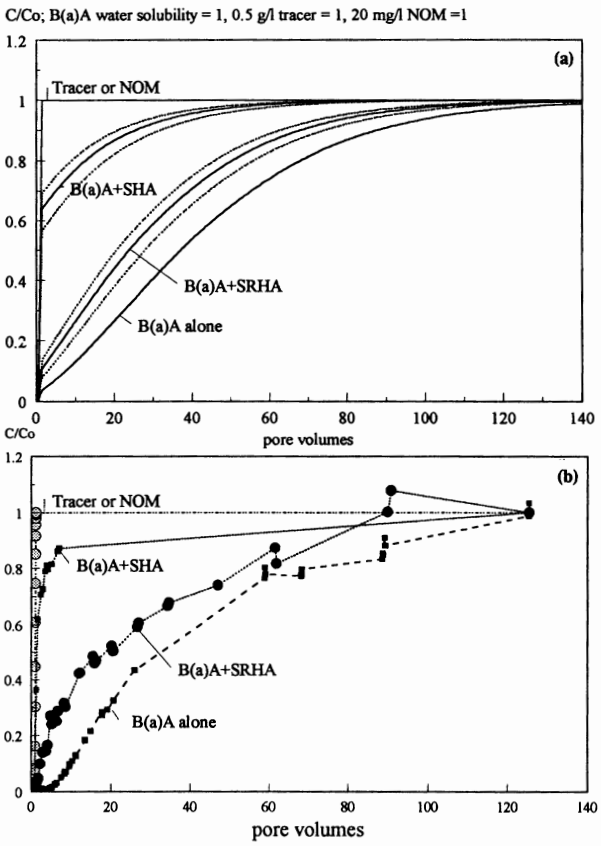

FIG. 2. B(a)A Facilitation through: (a) Quartz Model Simulations; (b) Experiment

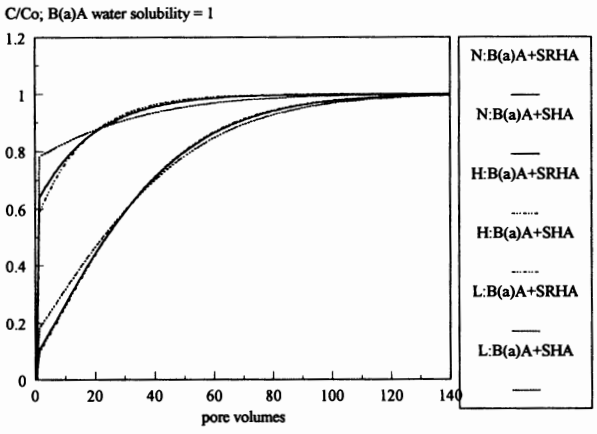

FIG. 3. B(a)A Facilitation through Quartz Model Simulations

ANALYSIS

Although the model itself does not require equilibrium conditions, our hypothesis is that use of mass-transfer coefficients derived from the equilibrium constants allowed, by comparison of model results to experimental data, determination of whether or not the physical processes in our experiments approached equilibrium. The values of the experimentally derived PAH-NOM association constants were matched against those reported in the literature (Johnson and Amy 1994) to show that they represented equilibrium. PAH-NOM interactions have been observed to reach completion within a few minutes (Schlautman 1992; Backhus 1990; Gauthier 1986), further supporting our observation. PAH-sediment interactions, however, may be subject to kinetic limitations over the course of our experiments, because they are observed to reach completion in times on the order of minutes to days (Ball and Roberts 1991; Schlautman 1992). PAH-sediment equilibration time has been shown to depend upon the nature of the sediment as well as the hydrophobicity of the PAH. The sediment used in our experiments is of low-organic-carbon content (f_{oc}). Sorption of perylene to bare silica was observed by Schlautman (1992) to require 2.5–4 hr to reach completion during batch experiments. NOM-sediment interactions have been observed to be kinetically controlled (Dunnivant et al. 1992), with initial rapid breakthrough followed by long tailing. Given the possible kinetic limitations on PAH and NOM interaction with sediment, further scrutiny of these processes was warranted. Experiments performed examining PAH interaction with quartz and composite nonmagnetic sediment were analyzed by CXTFIT, a curve-fitting algorithm by Parket and Van Genuchten (1984), which yields estimates of nonequilibrium parameters if the model is run in the nonequilibrium mode. The nonequilibrium parameters are BETA and OMEGA, which are the fraction of instantaneous retardation and the ratio of the hydrodynamic residence time to the characteristic time of sorption, respectively. A local equilibrium assumption is minimally violated for values of OMEGA greater than 4 (Brusseau et al. 1991). For the three simulations for experiments monitoring PAH breakthrough in quartz sediment, BETA was found to vary between 0.03 and 0.19, and OMEGA varied between 1.9 and 2.1. For experiments performed on composite nonmagnetic sediment, BETA varied between 0.00 and 0.50, and OMEGA varied between 1.1 and 9.7. The mean values of OMEGA are 2.03 for experiments in quartz sediment and 4.23 for experiments in composite nonmagnetic sediment (Table

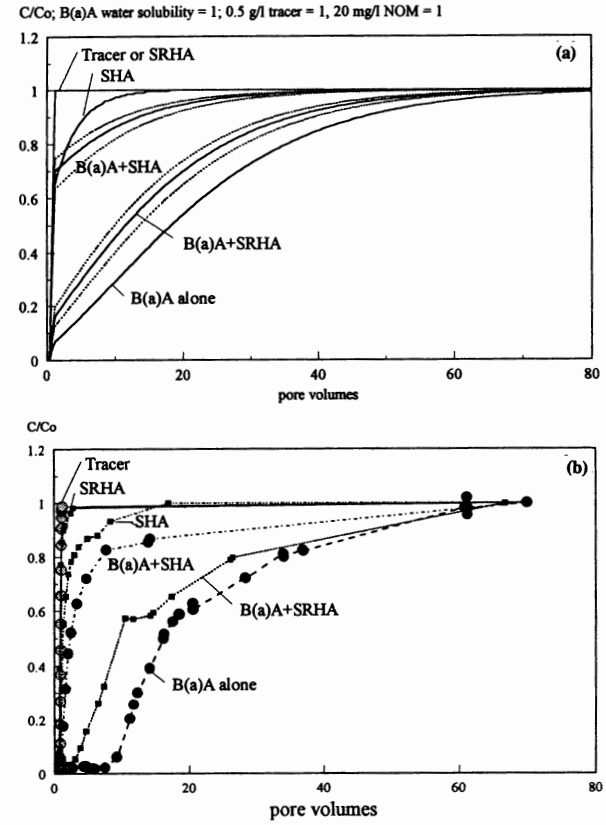

FIG. 4. B(a)A Facilitation through: (a) Nonmagnetic-Sediment Model Simulations; (b) Experiment

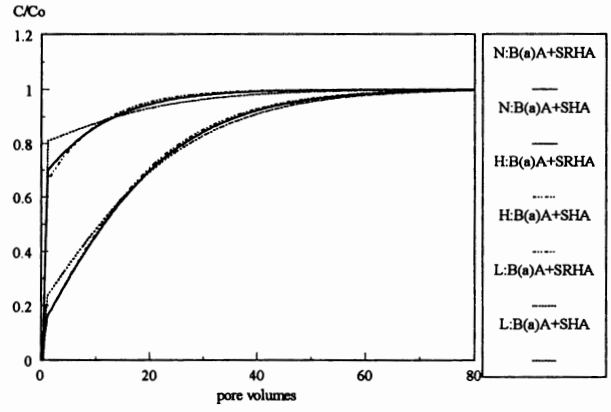

FIG. 5. B(a)A Facilitation through Nonmagnetic-Sediment Model Simulations

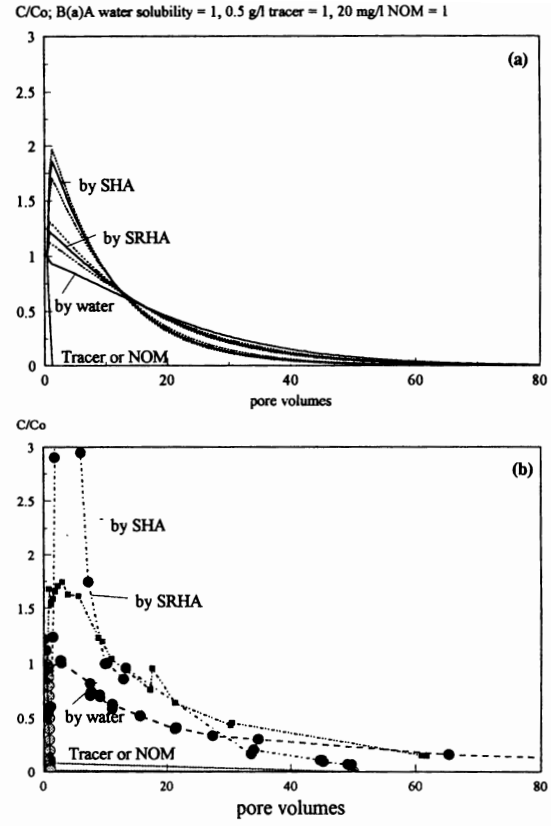

FIG. 6. B(a)A Enhanced Desorption from: (a) Quartz Model Simulations; (b) Experiment

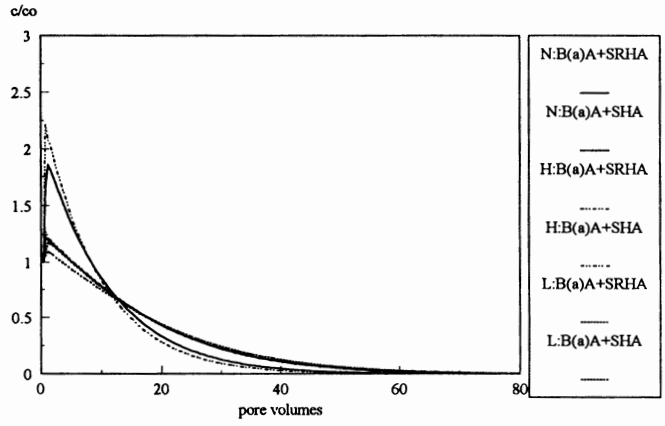

FIG. 7. B(a)A Enhanced Desorption from Quartz Model Simulations

5). Given that OMEGA equals 2 for experiments in quartz (and is probably 2 or above for experiments in nonmagnetic sediment) and that the local equilibrium assumption is minimally violated for values of OMEGA greater than 4, it appears that our observation that B(a)A transfer to and from our sediment is reasonably close to equilibrium may be corroborated by the CXTFIT simulations.

All mass-transfer ratios describing PAH-NOM, NOM-sediment, and PAH-sediment interactions were used as determined from experimental data except for slight adjustment of ratios of the mass-transfer coefficients for PAH and NOM transfer to and from nonmagnetic sediment. This is observed in Table 4, in which the magnitude ratios were changed slightly from unity to obtain a closer fit of the curves for breakthrough of PAH alone, and NOM alone, to the experimental data. Given the errors inherent in estimating K_d from experimental data, the use of a small adjustment should not be surprising. It must also be remembered that such adjustments were made on only two of the ratios.

The experimental data yielded only the ratios of the mass transfer coefficients, not their magnitudes. The magnitudes were increased equally to maintain the given ratio (except for the two slight adjustments described earlier). Because equilibrium is defined as equal mass transfer to and from a particular phase, the closer the mass-transfer–coefficient ratio was to unity, the more able that process was to achieve equilibrium over a variety of magnitudes. Table 4 shows the mass-transfer–coefficient ratios determined from experimental data, with the corresponding magnitudes. B(a)A-quartz and B(a)A–nonmagnetic sediment interactions both showed high deviation of their mass-transfer–coefficient ratios from unity relative to the other ratios. The other mass-transfer–coefficient ratios (PAH-NOM and NOM-sediment) yielded results that

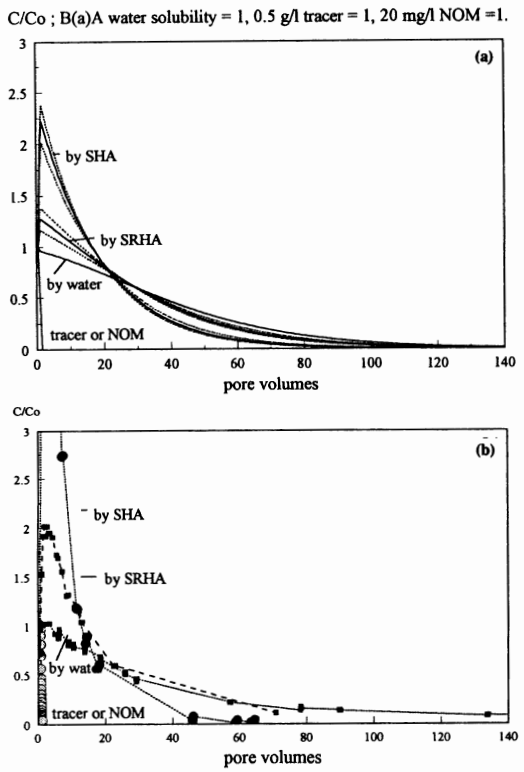

FIG. 8. B(a)A Enhanced Desorption from: (a) Nonmagnetic Sediment Model Simulations; (b) Experiment

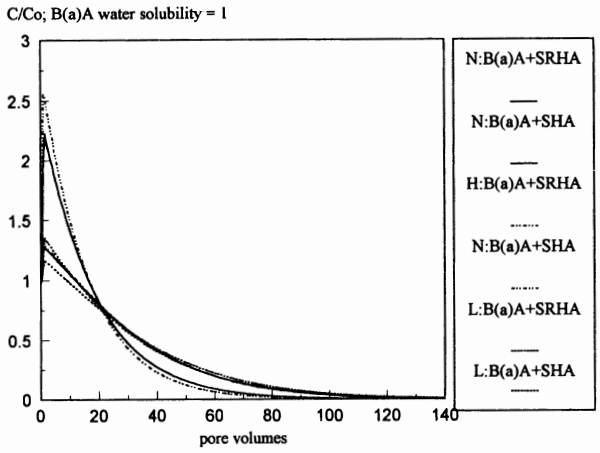

FIG. 9. B(a)A Enhanced Desorption from Nonmagnetic-Sediment Model Simulations

TABLE 5. Values of Nonequilibrium Parameters for Nonequilibrium Modeling of B(a)A BTC as Obtained from CXTFIT

Sediment (1)	BETA (2)	OMEGA (3)	Sum of squares of error (4)
Quartz	0.19	2.10	0.04
	0.16	1.90	0.14
	0.03	2.10	0.33
Nonmagnetic	0.30	1.90	0.02
	0.50	1.10	0.03
	0.00	9.70	0.01

matched the data over a variety of mass-transfer–coefficient magnitudes. This was because the mass-transfer–coefficient ratios were relatively close to unity, thereby ensuring equilibrium over a variety of magnitudes. The magnitudes of the B(a)A-quartz and B(a)A-sediment coefficients were increased to maintain their respective ratios until equilibrium was established (i.e., the magnitudes became sufficiently high that c_s/c_a became equal to K_d), it was observed that the model curves for B(a)A sorption alone to quartz or sediment matched the experimental curve for the same, indicating that B(a)A-quartz and B(a)A-sediment interactions were near equilibrium in our experiments. As the magnitudes of the coefficients were increased, the BTC changed shape and the total mass sorbed changed as well. Above a threshold magnitude, the total mass sorbed remained unchanged even as the magnitude of the coefficients was increased. This threshold magnitude represented attainment of equilibrium; i.e., the mass-transfer coefficients were of large enough magnitude (or the mass-transfer rate was high enough in both directions) that c_s/c_a equaled K_d. This is shown in Fig. 10, in which the coefficients that produce the best-fit BTC are 42.55 × 0.004 for $KPAH_{a-s}$ (where 42.55 is the numerator of the mass-transfer–coefficient ratio, and 0.004 is the magnitude by which this numerator is multiplied); and 1.0 × 0.004 for $KPAH_{s-a}$ (where 1.0 is the denominator of the mass-transfer–coefficient ratio, and 0.004 is the magnitude by which this denominator is multiplied). When the model was run with these coefficients in the absence of NOM, 6.26 μg of B(a)A were sorbed to the sediment. When the magnitudes of these coefficients were increased two orders of magnitude to 42.55 × 0.4 and 1.0 × 0.4, the mass of B(a)A adsorbed scarcely increased to 6.31 μg sorbed. In contrast, when the coefficients were decreased only slightly from the best-fit values to 42.55 × 0.001 ($KPAH_{a-s}$) and 1.0 × 0.001 ($KPAH_{s-a}$), the amount of B(a)A adsorbed decreased significantly to 5.54 μg.

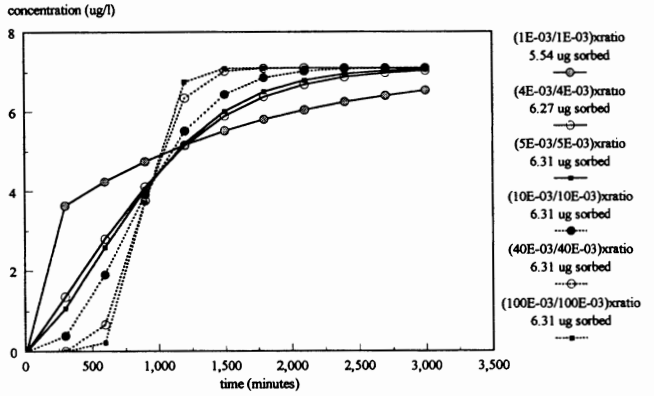

FIG. 10. Effect of Changing Magnitude on BTC (Ratio = $KPAH_{as}$/$KPAH_{sa}$ = 42.55/1)

Inclusion of the NOM phase and its associated mass-transfer coefficients (exactly as determined from experimental data) yielded the curves shown in our paper. The same parameters (without any change whatsoever) were then used to run the model in enhanced-desorption mode to yield the curves that compare very well to enhanced-desorption experiments. In addition to the magnitude of the mass-transfer coefficients, the ratio of the coefficients determines the shape of the BTC. Fig. 11 shows the effect of changing the ratio of the mass-transfer coefficients on the shape of the BTC. Thus, in addition to changing the magnitude of the coefficients, additional model runs were made with differing ratios of the coefficients to ensure that the determined ratio gave the best fit to the experimental data.

No distinct mechanism existed in the model to allow sediment-sorbed NOM to bind and release PAH. Sorbed NOM has been shown to have much less binding capacity for PAH relative to free NOM (Schlautman and Morgan 1993; Murphy et al. 1990). It was therefore assumed that the relatively small amount of sediment-sorbed NOM negligibly affected overall

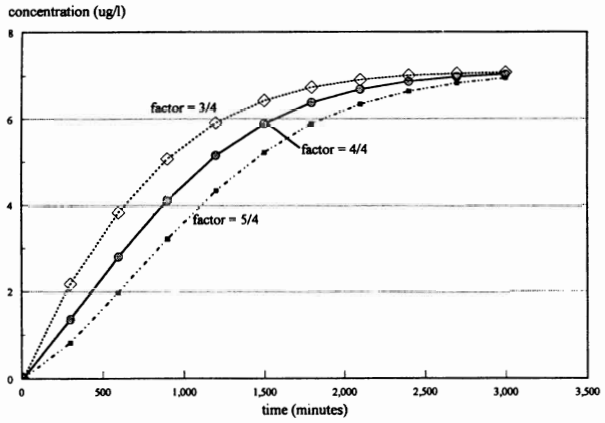

FIG. 11. Effect on BTC of Varying Ratio of Mass-Transfer Coefficients (Ratio = $KPAH_{as}/KPAH_{sa}$ = 42.55/1 was Multiplied by Various Factors Shown)

PAH sorption to sediment. Sorption of NOM by sediment, although assumed here to be relatively minor in its effect on sediment sorptivity toward PAH, was considered important to the aqueous-phase breakthrough of PAH, and so was included in the model. Our model was thus built on equilibrium constants that were readily determined from the experimental results. The success of the model in reproducing the experimental results indicated the proximity to equilibrium of the processes in our system. Possibly the binding of aqueous-phase PAH by NOM, which lowered the effective aqueous concentration of PAH, drove the diffusion of PAH from sediment so that desorption was much faster than is typically observed in the absence of NOM. This passive mechanism of enhancing PAH desorption implies that NOM might successfully enhance the desorption of hydrophobic contaminants from phases into which NOM cannot penetrate, for instance sediment micropores or other nonaqueous phases. The ability to do so would depend on the relative affinity of PAH for the impenetrable phase versus the aqueous NOM. The model was applied to a suite of low-organic-carbon aquifer sediments. Desorption of PAH from some sediments might be kinetically limited in the presence of NOM, depending upon the sediment organic matter content and conformation. An example of kinetically limited enhanced desorption of PAH by NOM is described in Johnson and Amy (1995).

CONCLUSIONS

The model successfully reproduced the facilitation and enhanced desorption effects of NOM on PAH transport observed in our experiments, thus indicating that facilitation and enhanced desorption are describable by interaction of the equilibrium constants that describe mass transfer of PAH between the various phases in our system. Despite the predominance of reports concerning nonequilibrium sorption and desorption of hydrophobic contaminants from soil, our own studies indicate that in our low-organic-carbon sediments, facilitation and enhanced desorption of PAH by NOM was not kinetically limited. Presumably the binding of aqueous PAH by aqueous NOM, with subsequent lowering of the effective aqueous PAH concentration, drove diffusion of PAH from sediment to a greater extent than is typically observed in the absence of NOM.

ACKNOWLEDGMENTS

This research has been supported by the Subsurface Science Program of the Ecological Research Division, Office of Health and Environmental Research, U.S. Department of Energy, Washington, D.C. (program director: Dr. F. J. Wobber).

APPENDIX. REFERENCES

Backhus, D. A. (1990). "Colloids in groundwater: Laboratory and field studies of their influence on hydrophobic organic contaminants," PhD dissertation, Massachussetts Inst. of Technol. (MIT), Cambridge, Mass.

Backhus, D. A., and Gschwend, P. M. (1990). "Fluorescent polycyclic aromatic hydrocarbons as probes for studying the impact of colloids on pollutant transport in groundwater." *Envir. Sci. and Technol.*, 24(8), 1214–1223.

Ball, W. P., and Roberts, P. V. (1991). "Long term sorption of halogenated organic chemicals by aquifer material." *Envir. Sci. and Technol.*, 25(7), 1223–1237.

Baum, E. J. (1978). "Occurrence and surveillance of polycyclic aromatic hydrocarbons." *Polycyclic aromatic hydrocarbons and cancer, Vol. 1*, H. U. Gelboin, and P. O. Ts'o, eds., Academic Press, New York, N.Y.

Brunauer, S., Emmett, P. H., and Teller, E. (1938). "Adsorption of gases in multimolecular layers." *J. Am. Chem. Soc.*, Vol. 60, 309.

Brusseau, M. L., Larsen, T., and Christensen, T. H. (1991). "Rate-limited sorption and nonequilibrium transport of organic chemicals in low organic carbon aquifer materials." *Water Resour. Res.*, 27(6), 1137–1145.

Brusseau, M. L., and Reid, M. E. (1991). "Non-equilibrium sorption of organic chemicals by low organic carbon aquifer materials." *Chemosphere*, 22(3/4), 344–350.

Callahan, M. A., et al. (1979). "Environmental fate of 129 priority pollutants." *EPA-440/4-79-029a,b*, U.S. Envir. Protection Agency, Washington, D.C.

Chiou, C. T., Malcolm, R. L., Brinton, T. I., Kile, D. E. (1986). "Water solubility enhancements of some organic pollutants and pesticides by dissolved humic and fulvic acids. *Envir. Sci. and Technol.*, 20(5), 502–508.

Chiou, C. T., Shoup, T. D., and Porter, P. E. (1985). "Mechanistic roles of soil humus and minerals in the sorption of nonionic organic compounds from aqueous and organic solutions. *Organic Geochem.*, 8(1), 9–14.

Corapcioglu, Y. M., and Jiang, S. (1992). "Colloid facilitated groundwater contaminant transport." *Water Resour. Res.*, 29(7), 2215–2226.

Dunnivant, F. M., Jardine, P. M., Taylor, D. L., and McCarthy, J. F. (1992). "Transport of naturally occurring dissolved organic carbon in laboratory columns containing aquifer material." *Soil Sci. Soc. of Am. J.*, Vol. 56, 437–444.

Enfield, C. G., Bengtsson, G., and Lindqvist, R. (1989). "Influence of macromolecules on chemical transport." *Envir. Sci. and Technol.*, 23(10), 1278–1286.

Gauthier, T. D., Shane, E. C., Guerin, W. F., Seltz, W. R., and Grant, C. L. (1986). "Fluorescence quenching method for determining equilibrium constants for polycyclic aromatic hydrocarbons binding to dissolved humic materials." *Envir. Sci. and Technol.*, 20(11), 1162–1166.

Grove, D. B., and Stollenwerk, K. G. (1984). "Computer model of one-dimensional equilibrium controlled sorption processes." *Water Resour. Investigations Rep. 84-4059*, U.S. Geological Survey.

Jardine, P. M., Dunnivant, F. M., Selim, H. M., and McCarthy, J. F. (1992). "Comparison of models for describing the transport of dissolved organic carbon in aquifer columns." *Soil Sci. Soc. of Am. J.*, 56(March/April), 393–401.

Johnson, W. P., and Amy, G. L. (1994). "Facilitated transport and enhanced desorption of polycyclic aromatic hydrocarbons (PAH) by natural organic matter (NOM) in aquifer sediments." *Environ. Sci. and Technol.*, 29(3), 807–817.

Karickhoff, S. W., Brown, D. S., and Scott, T. A. (1979). "Sorption of hydrophobic pollutants on natural sediments." *Water Res.*, 13(3), 241–248.

Liu, H., and Amy, G. L. (1993). "Modeling partitioning and transport interactions between natural organic matter and polynuclear aromatic hydrocarbons in groundwater." *Envir. Sci. and Technol.*, 27(8), 1553–1562.

Magee, B. R., Lion, L. W., and Lemley, A. T. (1991). "Transport of dissolved organic macromolecules and their effect on the transport of phenanthrene in porous media." *Envir. Sci. and Technol.*, 25(2), 323–331.

May, W. E. (1980). "The solubility of polycyclic aromatic hydrocarbons in aqueous systems." *Am. Chemical Soc. Adv. in Chem. Ser.*, 185(7), 143–192.

Mills, W. B., Liu, S., and Fong, F. K. (1991). "Literature review and model (COMET) for colloids/metals transport in porous media." *Ground Water*, 29(2), 199–207.

Murphy, E. M., Zachara, J. M., and Smith, S. C. (1990). "Influence of mineral-bound humic substances on the sorption of hydrophobic organic compounds." *Envir. Sci. and Technol.*, 24(10), 1507–1516.

Parker, J. C., and van Genuchten, M. T. (1984). "Determining transport parameters from laboratory and field tracer experiments." *Bull. 84-3*, Virginia Agric. Experiment Station, Blacksburg, Va.
Schlautman, M. A. (1992). "Mineral surfaces and humic substances: Partitioning of hydrophobic organic pollutants," PhD dissertation, California Inst. of Technol., Pasadena, Calif.
Schlautman, M. A., and Morgan, J. J. (1993). "Effects of aqueous chemistry on the binding of polycyclic aromatic hydrocarbons by dissolved humic material." *Envir. Sci. and Technol.*, 27(5), 961–969.
Thomann, R. V., and Mueller, J. A. (1987). *Principles of surface water quality modeling and control*. Harper & Row, Publishers, Inc., New York, N.Y.